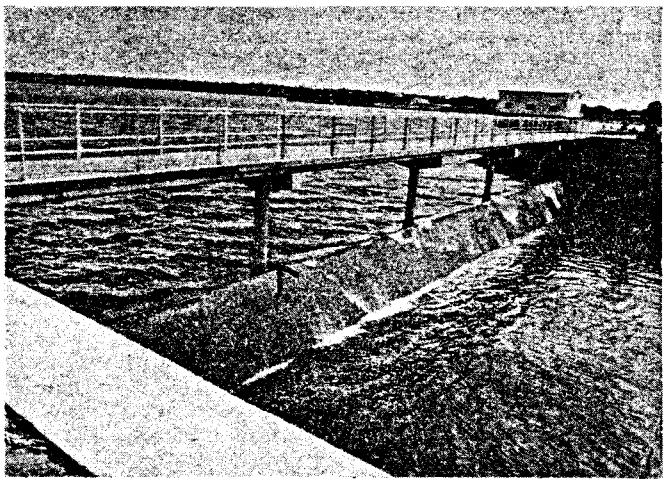

Bagoma dam spilling during the rainy season of July 1977.

of the five-band samples. The results obtained varied from 100 000 kg/m^2 to 210 000 kg/m^2. Compared with a figure of 700 000 kg/m^2 for solid hard granite, the results obtained were very low. It was essential, therefore, to remove a considerable portion of the schist bands. This was accomplished by removing a band about 6 m×30 m of the schist to an average depth of 3.5 m, where more competent rock was found. The part removed was replaced by mass concrete which formed the foundation for the spillway and thus eliminated the crushing of the weak schist under the spillway load and also improved the watertightness of the rock-spillway interface.

Intake pumping station. Construction of the intake pumping station posed several problems on site. As pointed out earlier, it was originally located behind the ogee spillway with its foundation assumed to be on rock because of the lack of adequate soil information. As a result of the increased dimensions of the dam, the intake had to be shifted upstream by about 30 m and it had to be enlarged to accommodate more pumps which were required by the additional demand for domestic supplies and irrigation. The change of location made it necessary for the intake structure to be moved to within 20 m of the extremely pervious cofferdam, causing incessant water seepage through this dam into the intake foundation.

Dewatering had to be carried out all day long using petrol and diesel pumps, so that the foundation excavation and concreting could take place. About 1125 l of diesel were consumed per day during the dewatering exercise. At the new location, the foundation of the intake was not the assumed rock but dense alluvial sand with a bearing capacity of 80 kN/m^2. The foundation was hence redesigned as a raft foundation, the contact pressure of which was 50 kN/m^2. The raft had a thickness of 1.25 m to counter the effect of buoyancy.

A 2 m-wide and 30 m-long bridge, supported on asbestos cement pipes filled in with concrete, linked the pumping station to the crest of the dam.

Post constructional use

The project was commissioned in 1976 after the necessary trial run of all the equipment. The town of Birnin Gwari is now receiving 600 m^3 of potable water a day. Nothing is being supplied to Kusheriki. The 4500 m^3/day allocated to the town may be used to increase the demand to Birnin Gwari or to irrigate more farmland, or both.

At the commissioning of the scheme, the land to be irrigated had not been allotted. By now, however, out of the 400 ha of farmland designed to be irrigated, 15 ha is already receiving water at the average rate of 1500 m^3/day during a six-month growing season. The photograph opposite shows the full lake spilling during the middle of the 1977 rainy season. □

Acknowledgment
The author wishes to express his deep gratitude to the Kaduna State Water Board and the Kaduna State Ministry of Agriculture and Natural Resources for permission to use materials included in the article.

Modern trends in selecting and designing reversible Francis pump-turbines

By F. de Siervo and A. Lugaresi
Chief* and Senior Engineer*

This paper presents the result of an extensive statistical investigation made on 80 Francis-type reversible pump-turbines manufactured throughout the world, to provide engineers with an up-to-date reference source for preliminary design at the feasibility study stage.

THE INSTALLATION of large thermal and nuclear power stations in developed countries has increased the demand for peak capacity in recent years. This is required both for smoothing the load diagram of steam powerplants to improve their utilization, and for covering unpredictable failures of large units, thus increasing the reliability of electric power systems. The progressive exhaustion of the most economical hydraulic resources in developed countries has led to the adoption of pumped-storage plants. These facilitate steady loading of steam powerplants by storing energy during low demand periods and provide a reliable, relatively simple and promptly available peak capacity.

The present study is limited to Francis-type single-stage reversible pump-turbines, the hydraulic machines most widely adopted in pumped-storage projects.

The research detailed in this article covers, with a few exceptions, the period between 1961 and 1977. The units

* Hydromechanical Department Electroconsult, 20151 Milan, Italy.

examined cover the head range of 20-600 m, with capacities up to 400 MW. The Table gives the main features of the installations investigated taken from the published information while the diagrams are based on the project data and dimensions collected by an extensive inquiry similar to that made for conventional turbines[1,2,3]. The curves are drawn by the same simple regression procedure adopted in the previous articles. General considerations, common to reversible and conventional Francis turbines, are omitted for simplicity; the authors suggest that a better understanding of this subject will be achieved by referring to the previous article[1].

General selection criteria

The design of a pumped-storage scheme involves many and often complex considerations based on the nature of the site selected, the requirements of the electric network and the characteristics of the units.

As a result, a preliminary operating schedule for pumping and generation is obtained together with the duration curves of the head and the desirable values of turbine and pump capacity.

The engineer is then required to refine these preliminary calculations harmonizing the mutually contradictory pump and turbine performances with the aim of obtaining the maximum mean efficiency of the system.

This result can be achieved only on the basis of the complete diagram of characteristics for the machine, which is usually not available during the preliminary design. The statistical diagrams presented in this study provide reliable information on the main characteristics and dimensions of reversible units for the preliminary planning mentioned above.

Usually the main data available when selecting the reversible unit are: maximum, rated, and minimum net heads for the turbine and pump modes of operation, rated turbine capacity and a desired ratio between the pump and turbine capacities. The same characteristic constant used for conventional Francis turbines is adopted for the reversible pump-turbine in both modes of operation:

$$n_s = n\, P^{0,5}\, H^{-1,25} \qquad \ldots \quad (1)$$

and the statistical relationship:

$$n_s = n_s\,(H)$$

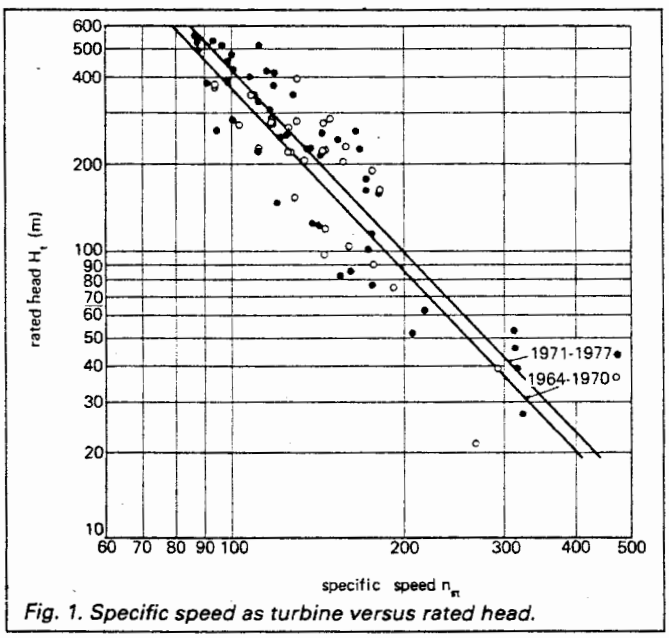

Fig. 1. Specific speed as turbine versus rated head.

Main features of some reversible Francis units installed after 1961

Powerplant	Turbine manufacturer*	Year	Turbine operation		
			Head (m)	Output (MW)	Rotational frequency (rev/min)
Aguiera	Nohab	1978	61.1	90	125
Aurland III	Kvaerner Brug	1975	400	150	500
Azumi	Toshiba	1968	134.9	108.5	187.5
Bad Creek	Allis Chalmers	1976	309	257	300
Bajina Basta	Toshiba	1976	600.3	315	428.6
Bath County	Allis Chalmers	1976	329	380	257.1
Bendeela	Voest-Alpine	1971	116	41	333.3
Bolarque	Escher-Wyss	1969	258.1	56.65	600
Brasimone	Riva Calzoni[2]	1970	377.7	169.7	375
Brasimone	Escher Wyss[2]	1970	377.7	169.7	375
Camlough	KMW Boving	1972	158	117	300
Caplina	Riva	1974	227	245.64	300
Carters	Allis Chalmers	1968	105	129	150
Chong Pyong	Fuji[4]	1976	452	206	450
Clarence Cannon	Allis Chalmers	1968	23	32	75
Conso	Escher Wyss	1971	230	91	375
Coo-Trois Ponts I	Allis Chalmers	1966	270	145	300
Coo-Trois Ponts II	Allis Chalmers Voith[3]	1975	275	210	272.7
Cruachan	KMW Boving	1961	342	102	500
Dinorwic	KMW Boving	1975	513	302	500
Drakensberg	Toshiba	1977	422	269	375
Duge	Kvaerner Brug	1974	215	100	375
Estangento	Voith	1976	370	104	600
Fairfield	Allis Chalmers	1972	46	62	150
Folgefonnverkene Jukla	Kvaerner Brug	1970	240/70	47	500/375
Foyers	KMW Boving	1969	163	152.4	273
Gabriel y Galan	Voith	1977	59	110	136.36
Gosau III	Voith	1972	150	70	750
Grand Coulee	Nohab	1970	110.3	50.3	200
Grand Coulee	Toshiba	1977	85.6	44.5	200
Guillena	KMW	1969	230	71.7	375
Hatanagi I	Fuji	1972	83.5	38.8	200
Hongawa	Mitsubishi	1977	530	307	400
Horse Mesa	BLH/Voest-Alpine	1969	75	80	150
Jocassee	Allis Chalmers	1967	90	170	120
Juktan	KMW Nohab	1973	260	333.6	300
Kadamparai	KMW Boving	1974	341	102	500
Kalayaan	Hydroart	1977	282	154.05	300
Kisenyama	Toshiba	1968	220	240	225
Kühtai	Voith	1977	430	148	600
Langenprozelten	Voith	1972	310	88	500
La Plate Taille	Escher Wyss	1973	47	35	166.7
Le Chylas	Neyrpic[5]	1979	256.2	251.5	300
Mloty	Toshiba	1978	247.6	257	300
Mormon Flat	Allis Chalmers	1968	39	42	138.5
Mt. Elbert	Allis Chalmers	1971	123	103	180
Mount Elbert	Toshiba	1976	124	103	180
Northfield	BLH/Voest-Alpine	1967	227	250	257
Oberberg II	Voith	1975	256	4.4	1500
Obrovac	Voith	1978	517	140	600
Oeljusioeen	Kvaerner Brug	1972	220	50	428.6
Ohira	Toshiba	1972	512	256	400
Okutataragi	Mitsubishi	1972	387.6	310	300
Okuyahagi I	Toshiba	1977	161	107.3	300
Okuyoshino	Toshiba	1974	526	207	514
Parabka-Zar	KMW Boving	1971	420	135	600
Raccoon Mt.	Allis Chalmers	1970	287	347	300
Revin	Neyrpic[6]	1970	240	200	300
Rio Grande	Allis Chalmers	1974	178	204	250
Rodund II	Voith	1971	348	271	375
Rönkhausen	Escher Wyss	1964	274	74.7	500
Saint Croix	Neyrpic[6]	1971	77	59	166.7
Santiago del Jares	KMW	1964	217	26.6	500
Savalen	Kvaerner Brug	1968	220	62.5	428
Shintakasegawa	Mitsubishi	1973	241.7	336	214
Shintoyone	Toshiba	1971	236	230	257
Shiroyama	Toshiba	1965	181.5	65	273
Smith Mt III	Allis Chalmers	1975	52	103	90
Tajo de la Encantada	Neyrpic[7]	1972	398	92	500
Takasegawa	Toshiba	1975	241.7	336	214
Taloro	Riva[1]	1970	311.4	88.1	500
Taloro	Escher Wyss[2]	1971	314	90.7	500
Tamakara	Mitsubishi	1978	518	309	429
Tanes	Neyrpic[7]	1972	123	66.5	250
Turlough-Hill	KMW	1969	287	80.7	500
Vianden X	Escher Wyss[8]	1970	287.1	196.4	333.3
Villarino	KMW Boving	1966	386	138	600
Wallace Dam	Allis Chalmers	1971	27	54	85.8

* In cooperation with: (1) De Pretto-Escher Wyss; (2) Riva Calzon's; (3) Cockerill; (4) Allis Chalmers and Nissho-Iwai; (5) Creusot-Loire; (6) Creusot-Loire and Jeumont-Schneider; (7) Neyrpic Spain; and, (8) Voith.

is sought between the specific speed and the rated head. The available data have been divided into two groups, depending on the year of design of the machines. This gives the regression curves indicated in Figs. 1 and 2 respectively for the turbine and pump operation. The interpolating functions are:

1961-1970 $\quad n_{st} = 1700\, H_t^{-0.481}$

$\qquad\qquad n_{sp} = 1672\, H_p^{-0.480}$

1971-1977 $\quad n_{st} = 1825\, H_t^{-0.481}$

$\qquad\qquad n_{sp} = 1768\, H_p^{-0.480}$ $\qquad \ldots \quad (2)$

The correlation coefficients and the standard deviations are respectively:

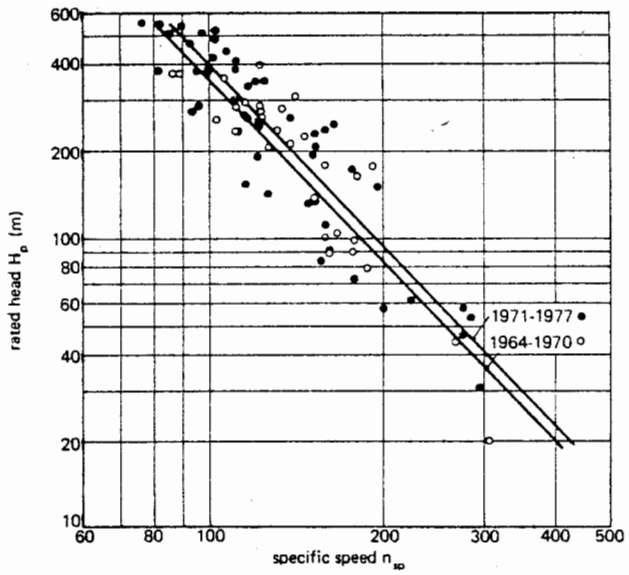

Fig. 2. Specific speed as pump versus rated head.

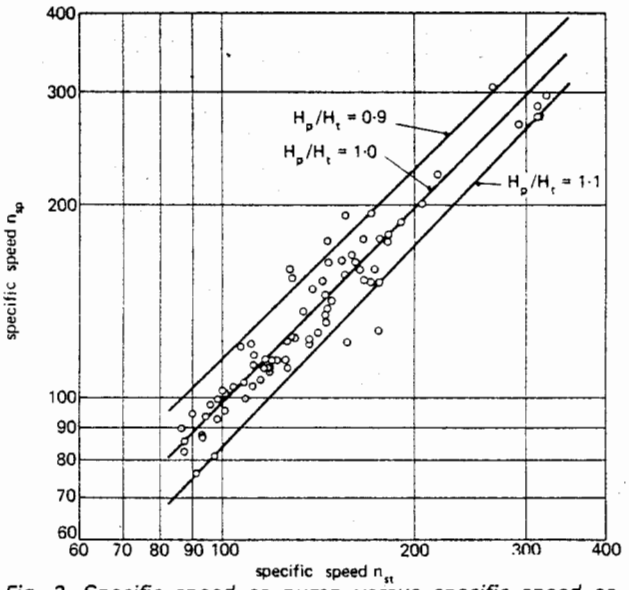

Fig. 3. Specific speed as pump versus specific speed as turbine.

r=−0.85	r=−0.90	r=−0.91	r=−0.91
s=68.8	s=67.5	s=76.6	s=78.9

The trend to increasing n_s values for a given head from the first to second period chosen is evident but less pronounced than for conventional Francis turbines. Difficulties in harmonizing pump and turbine performances in reversible machines probably justify this reduced difference.

The strict correlation between the characteristics in the pump and turbine modes is shown by Fig. 3, where n_{sp} is plotted against n_{st} for different ratios of the pump and turbine rated heads.

The interpolating functions are:

$$H_p/Ht=0.9 \qquad n_{sp}=1.272\ n_{st}^{0.978}$$
$$H_p/Ht=1.0 \qquad n_{sp}=0.842\ n_{st}^{1.033}$$
$$H_p/Ht=1.1 \qquad n_{sp}=0.619\ n_{st}^{1.065}$$

with:

Notations

g	= gravity acceleration (m/s²)
h_b	= barometric pressure (m)
h_s	= static suction head referred to the wicket gates centreline (m)
h_w	= water vapour pressure (m)
n	= pump-turbine frequency of rotation (rev/min)
n_f	= pump-turbine runaway frequency of rotation (rev/min)
n_{sp}	= actual specific speed in pumping mode
$\bar{n}_{sp}$	= statistical specific speed in pumping mode
n_{st}	= specific speed in generating mode
r	= statistical curve correlation coefficient
s	= statistical curve standard deviation
v_{ip}	= water velocity at runner inlet in pumping mode (m/s)
v_{op}	= water velocity at spiral casing outlet in pumping mode (m/s)
D_1	= runner diameter at guide vanes centreline (m)
H_p	= rated head as pump (m)
H_{pm}	= minimum head as pump (m)
H_{pM}	= maximum head as pump (m)
H_t	= rated head as turbine (m)
K_{vip}	= ratio between water velocity v_{ip} and spouting velocity
K_{vop}	= ratio between water velocity v_{op} and spouting velocity
K_u	= runner peripheral velocity coefficient
P_p	= rated capacity as pump (kW)
P_{pM}	= maximum capacity as pump (kW)
P_t	= rated capacity as turbine (kW)
λ	= relative capacity variation
σ	= actual cavitation coefficient
$\bar{\sigma}$	= theoretical cavitation coefficient

For notations relevant to the machine main dimensions, refer to the relevant figures.

r=0.97	r=0.96	r=0.99
s=12.9	s=14.9	s=11.5

Since the rated generating capacity represents usually the most significant network requirement, the frequency of rotation of the unit is determined by starting from the turbine ratings.

Referring to the diagram in Fig. 1, with the rated head H_t, the turbine specific speed n_{st} is obtained and the best rotation frequency is calculated using Eq. (1). The rated frequency of the machine will coincide with one of those synchronous frequencies which is nearest the ideal one, depending on considerations similar to those indicated for conventional Francis turbines[1].

The final value of n_{st} will be then calculated applying Eq. (1) again.

The pump specific speed n_{sp} is determined from the diagram in Fig. 3, entering n_{st} on the curve relevant to the actual ratio H_p/H_t.

Applying Eq. (1) again, the rated pump capacity P_p is determined and the Ratio P_p/P_t is calculated. If this ratio differs substantially from the desired one, a new selection of n_{sp} is made on the diagram, adopting a different value

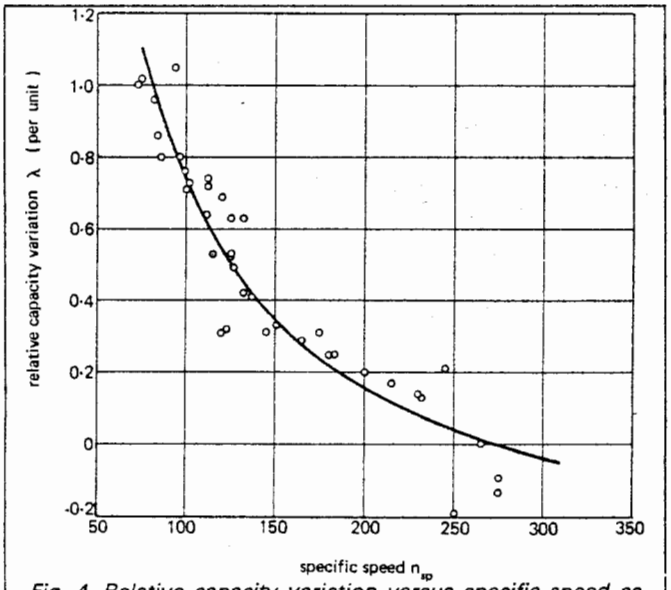

Fig. 4. Relative capacity variation versus specific speed as pump.

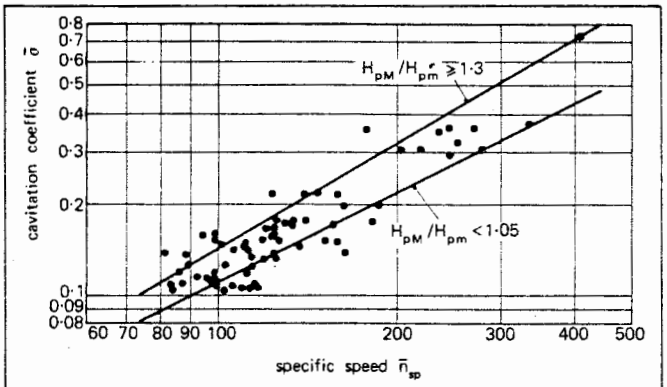

Fig. 5. Theoretical cavitation coefficient versus statistical specific speed as pump.

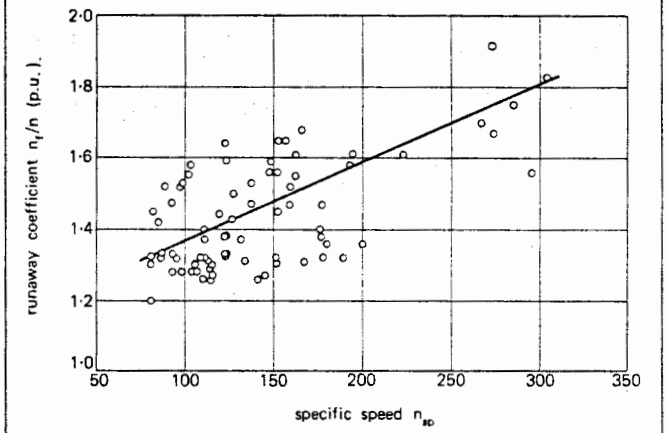

Fig. 6. Ratio between runaway and rated frequencies of rotation versus specific speed as pump (as in the following drawings, p.u. = per unit).

of the pump rated head H_p.

To evaluate the capacity of the synchronous motor-generator, it is necessary to determine the maximum capacity in pumping mode. Depending on the pump specific speed, the maximum capacity is attained at minimum or maximum net pumping head.

Fig. 4 gives the capacity variations $\Delta P_p/P_p$, referred to the head variations $\Delta H_p/H_p$, against pump specific speed n_{sp}. The diagram shows that for $n_{sp} \leqslant 275$, the maximum capacity is attained at minimum head ($\Delta H_p = H_p - H_{pm}$), while for $n_{sp} > 275$, the maximum capacity is attained at maximum head ($\Delta H_p = H_p - H_{pM}$). The maximum capacity is given by the following equation:

$$P_{pM} = P_p(1 + \lambda \Delta H_p/H_p)$$

in which

$$\lambda = -0.417 + 114.70/n_{sp}$$

is the interpolating function of the points indicated in Fig. 4. These have been obtained from existing machines, linearizing their capacity-head curves around the operating point at rated head.

The correlation coefficient and the standard deviation are:

$$r = 0.94 \qquad s = 0.11$$

The cavitation coefficient σ for reversible machines is expressed by the same formula adopted for conventional Francis turbines:

$$\sigma = (h_b - h_w - h_s)/H_p \qquad \ldots \quad (3)$$

This coefficient depends mainly on the pump specific speed n_{sp}, the rated head H_p and the ratio H_{pM}/H_{pm} between maximum and minimum pumping heads. The available data lead to the following regression curves:

$$H_{pM}/H_{pm} < 1.05 \qquad \tilde{\sigma} = 0.00122 \tilde{n}_{sp}^{0.982}$$

$$H_{pM}/H_{pm} \geqslant 1.30 \qquad \tilde{\sigma} = 0.000712 \tilde{n}_{sp}^{1.15}$$

with:

$$r = 0.96 \qquad s = 0.034 \qquad r = 0.93 \qquad s = 0.050$$

In these equations $\tilde{n}_{sp}$ represents the statistical specific speed corresponding to the rated head H_p, according to Eq. (2), and takes into account the previously mentioned influence of Hp. The influence of the actual specific speed n_{sp} on the cavitation coefficient σ is considered by the formula;

$$\sigma = \tilde{\sigma}(n_{sp}/\tilde{n}_{sp})^{1.25} \qquad \ldots \quad (4)$$

For each case, the value of $\tilde{n}_{sp}$ is first determined using Eq. (2); then the value of $\tilde{\sigma}$ is sought from Fig. 5, entering $\tilde{n}_{sp}$ on the curve corresponding to the actual value of H_{pM}/H_{pm}.

The value of σ is calculated from Eq. (4) inserting a value for the ratio between actual and statistical specific speed values and finally, the submergence H_s is obtained from Eq. (3).

Comparing σ values of reversible machines with those of conventional Francis ones[1], it can be seen that submergences for reversible units are much larger, reaching values even greater than 60 m for high-head plants.

The ratio of the steady-state turbine runaway frequency of rotation to the rated one, necessary to define the design of the motor-generator, is expressed as a function of n_{sp} in Fig. 6. All the available data are referred to the rated turbine head H_t and to the maximum guide vane opening.

The interpolating function is:

$$n_f/n = 1.153 + 0.00215\, n_{sp} \qquad \ldots \quad (5)$$

with:

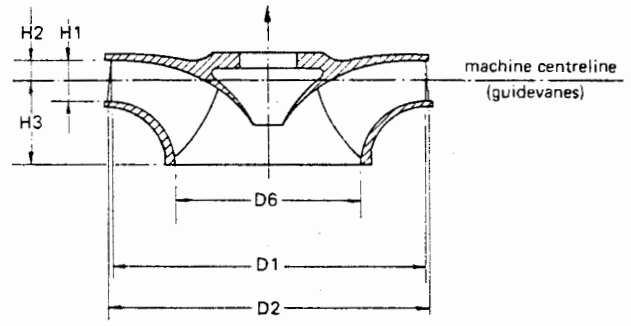

Fig. 7. Main dimensions of the runner.

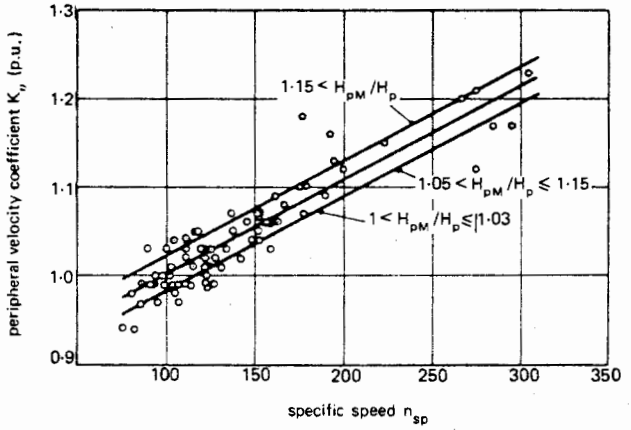

Fig. 8. Runner peripheral velocity coefficient versus specific speed as pump.

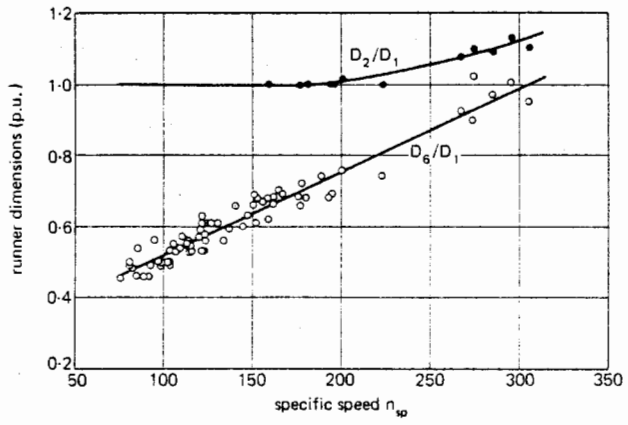

Fig. 9. Main runner dimensions versus specific speed for the ratios D_2/D_1 and D_6/D_1.

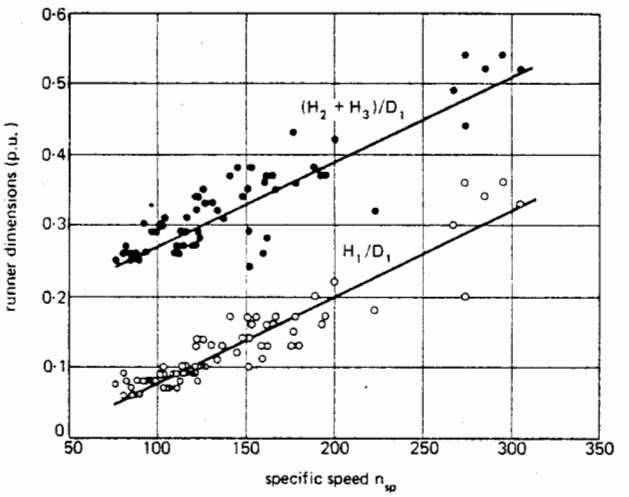

Fig. 10. Main runner dimensions versus specific speed for the ratios $(H_2 + H_3)/D_1$ and H_1/D_1.

r=0.49 s=0.25

For powerplants with considerable head variations, a first approximation value for n_f can be obtained by increasing the value given by Eq. (5) proportionally to the square root of the ratio H_M/H_t. It is worth mentioning that reversible units may attain transient runaway frequencies of rotation higher than the values given by Eq. (5) in the event of a trip-out during pumping or generation.

All the design elements given in this section represent a compromise solution for the data available and should be used with some degree of caution, keeping in mind that they cannot substitute the characteristic diagram for the machine. In particular the diagram in Fig. 4 may only be considered fully reliable, within the standard deviation range indicated, if the actual capacity-head curves are straight lines.

It is worth mentioning that the presence of possible instability phenomena in pumping mode may condition the actual choice of the operating range of the machine, particularly at high heads.

Runner size

The runner main dimensions are determined by the peripheral velocity coefficient K_u:

$$K_u=\pi\, D_1 n/(60\sqrt{[2g\, H_p]}) \quad \ldots \quad (6)$$

in which D_1 is the runner diameter indicated in Fig. 7. K_u depends upon the pump specific speed and the ratio H_{pM}/H_p between maximum and rated pumping heads. The dependence on H_{pM}/H_p, evident in the available data, originates from the necessity to guarantee that the pump is capable of delivering the requested flow under the maximum head.

Fig. 8 shows the available data and gives the resulting interpolating functions:

$$\begin{aligned} &1<H_{pM}/H_p\leq 1.03 && K_u=0.875+1.07\times10^{-3}n_{sp}\\ &1.05<H_{pM}/H_p\leq 1.15 && K_u=0.895+1.07\times10^{-3}n_{sp}\\ &1.15<H_{pM}/H_p && K_u=0.915+1.07\times10^{-3}n_{sp} \end{aligned} \quad \ldots \quad (7)$$

with, respectively:

r=0.96 r=0.92 r=0.79
s=0.022 s=0.021 s=0.029

Once K_u is determined from Eqs. (7), the diameter D_1 is calculated from Eq. (6).

The other runner dimensions indicated in Fig. 7 may be obtained as a function of n_{sp}, referred to the diameter D_1, from the curves in Figs. 9 and 10.

The interpolating functions of the various curves are:

$$\begin{aligned} &D_6/D_1=0.284+0.00235\, n_{sp}\\ &D_2/D_1=1.0 && n_{sp}\leq 190\\ &D_2/D_1=1/(1.198-0.00104\, n_{sp}) && n_{sp}>190\\ &H_1/D_1=-0.0438+0.00121\, n_{sp}\\ &(H_2+H_3)/D_1=0.155+0.00119\, n_{sp} \end{aligned}$$

with respectively:

r=0.97 r=−0.87 r=0.93 r=0.89
s=0.032 s=0.015 s=0.024 s=0.034

The values of r and s obtained indicate that, as far as the runner size is concerned, the design criteria of the different manufacturers are very similar.

Spiral casing size

The dimensions of the spiral case depend essentially on the value assumed for the water velocity at the outlet section.

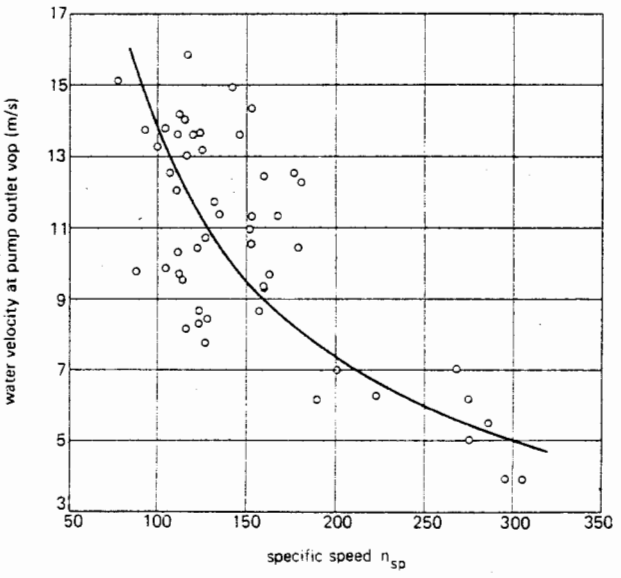

Fig. 11. Water velocity at spiral casing outlet in pumping mode versus specific speed as pump.

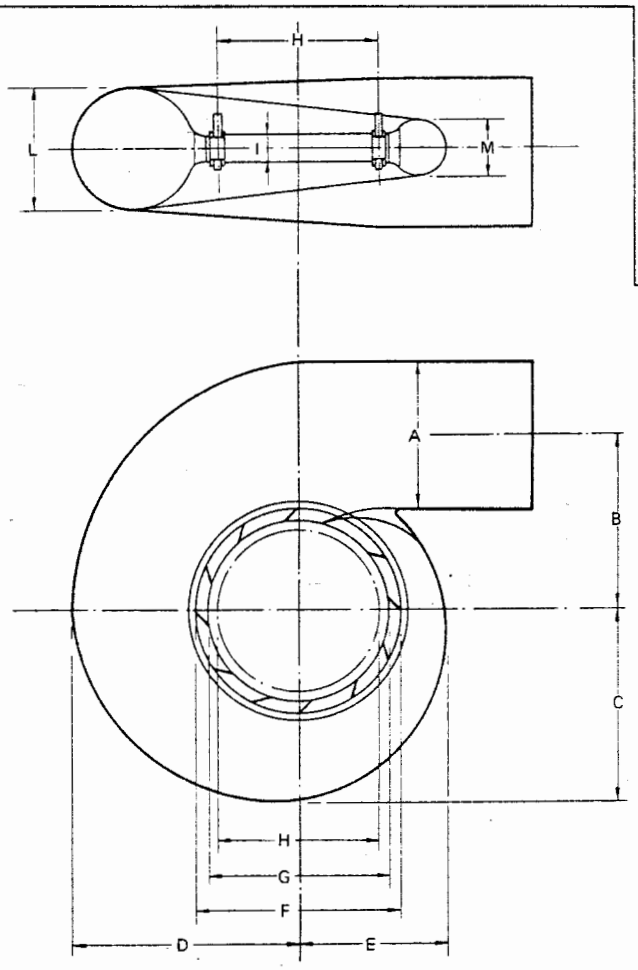

Fig. 12. Main dimensions of the spiral casing.

Fig. 11 gives, as a function of n_{sp}, the average statistical value of the absolute water velocity at the outlet section of the spiral case. The interpolating function is:

$$v_{op}=1/(0.00943+0.000641\ n_{sp})$$

r=0.82 s=2.44

Comparing Fig. 11 with the diagram of the water velocity at spiral case inlet for conventional Francis turbines[1], it appears that for high heads the water velocity is higher for pump-turbines in pumping mode. This difference becomes more pronounced in the generating mode, being the result of a technical compromise between these two opposing requirements:

- to adopt high velocities in the pumping mode to improve the stability of the flow, with the aim of increasing efficiencies and minimizing the instability of the pump characteristic, which is more evident at high heads; and,
- to adopt low velocities in the generating mode to minimize the spiral case head losses.

The main dimensions of the spiral case indicated in Fig. 12 may be obtained as a function of n_{sp}, referred to the diameter D_1, from the curves of Figs. 13 to 21.

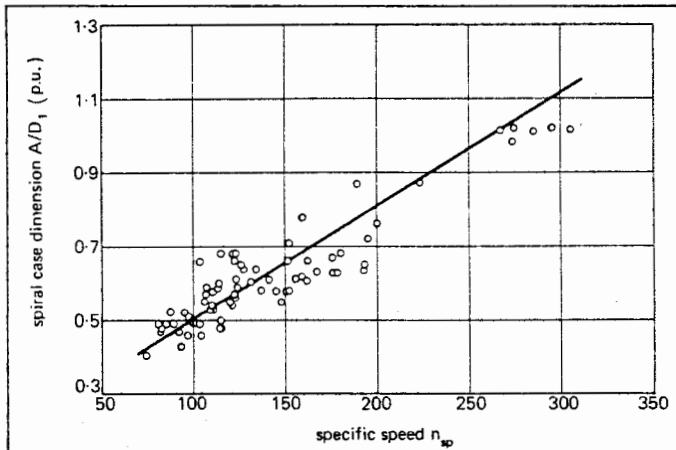

Fig. 13. Specific speed versus main spiral case dimensions A/D — pump.

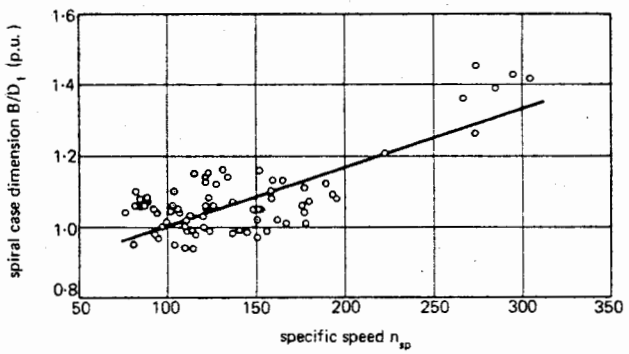

Fig. 14. Specific speed versus main spiral case dimensions B/D_1 — pumping mode.

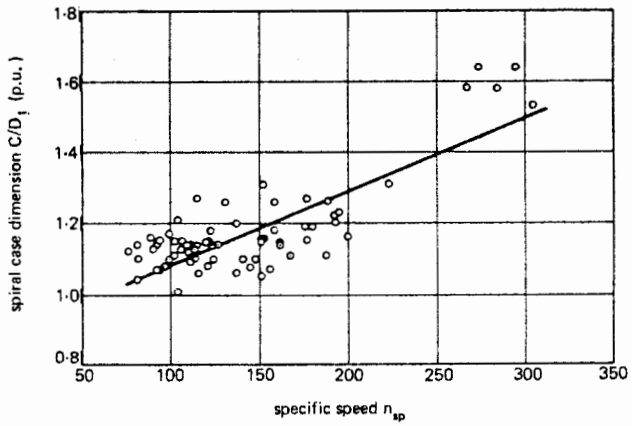

Fig. 15. Specific speed versus main spiral case dimensions C/D_1 — pumping mode.

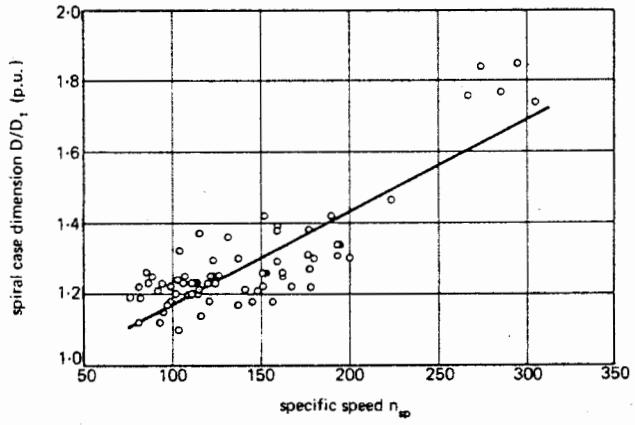

Fig. 16. Specific speed versus main spiral case dimensions D/D_1 — pumping mode.

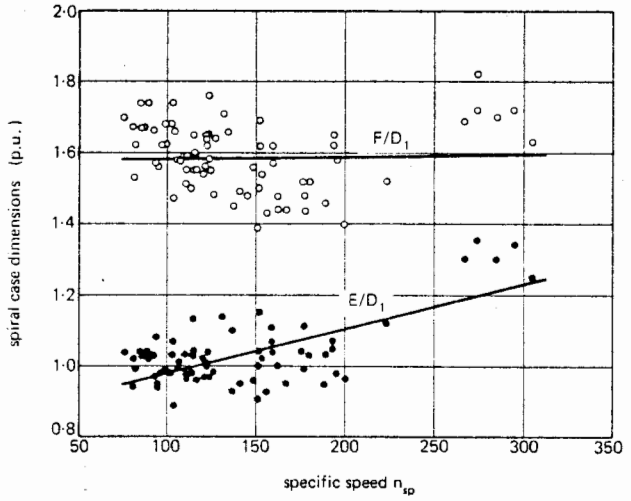

Fig. 17. Specific speed versus main spiral case dimensions F/D_1 and E/D_1 — pumping mode.

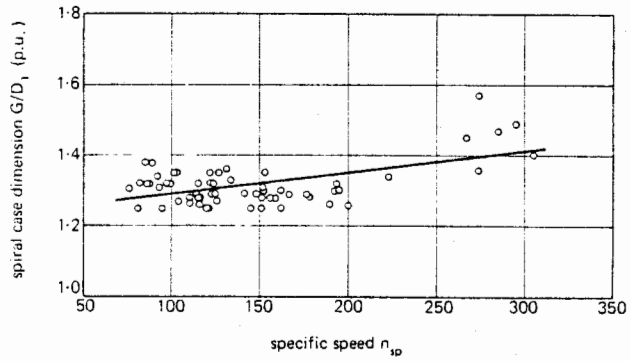

Fig. 18. Specific speed versus main spiral case dimensions G/D_1 — pumping mode.

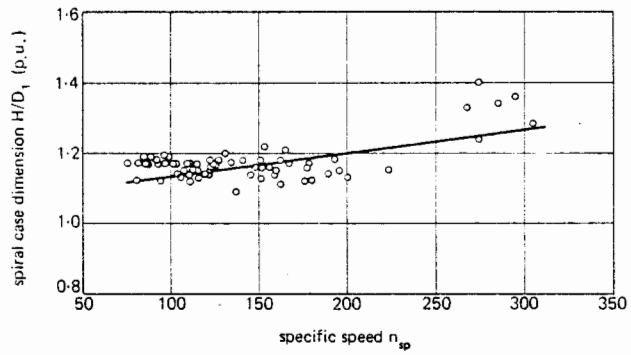

Fig. 19. Specific speed versus main spiral case dimensions H/D_1 — pumping mode.

The interpolating functions for the different curves are as follows:

$$A/D_1=0.19+0.0031\ n_{sp}$$

r=0.92 s=0.070

$$B/D_1=0.84+0.0016\ n_{sp}$$

r=0.78 s=0.069

$$C/D_1=0.88+0.0020\ n_{sp}$$

r=0.81 s=0.077

$$D/D_1=0.91+0.0026\ n_{sp}$$

r=0.86 s=0.082

$$E/D_1=0.86+0.0012\ n_{sp}$$

r=0.69 s=0.069

$$F/D_1=1.58+0.000072\ n_{sp}$$

r=0.04 s=0.094

$$G/D_1=1.23+0.0006\ n_{sp}$$

r=0.55 s=0.051

$$H/D_1=1.084+0.00061\ n_{sp}$$

r=0.58 s=0.042

$$I/D_1=-0.041+0.0012\ n_{sp}$$

r=0.95 s=0.021

$$L/D_1=0.21+0.0022\ n_{sp}$$

r=0.86 s=0.053

$$M/D_1=0.12+0.0013\ n_{sp}$$

r=0.87 s=0.03

The ratio K_{vop} between the water velocity v_{op} at spiral case outlet and the spouting velocity corresponding to the rated head, obtained from Figs. 2 and 11, is shown in Fig. 22.

Examining the corresponding diagram given for Francis turbines[1], it can be seen that for pump-turbines the range of K_v is smaller. This indicates a tendency for the incidence of the head losses compared with the total head to remain constant as n_s increases.

Draft tube size

The draft tube dimensions are directly related to the runner size and to the absolute velocity at its inlet section.

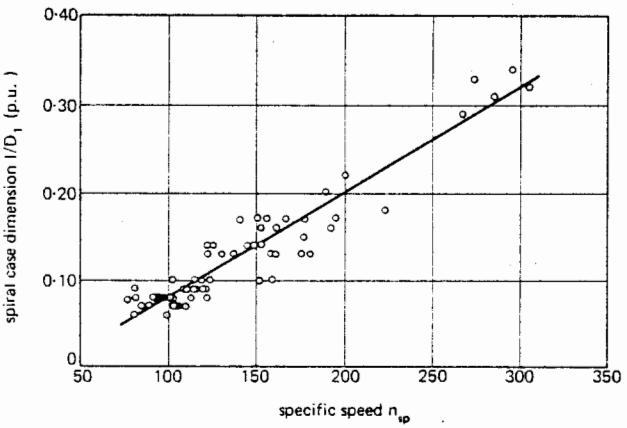

Fig. 20. Specific speed versus main spiral case dimensions I/D_1 — pumping mode.

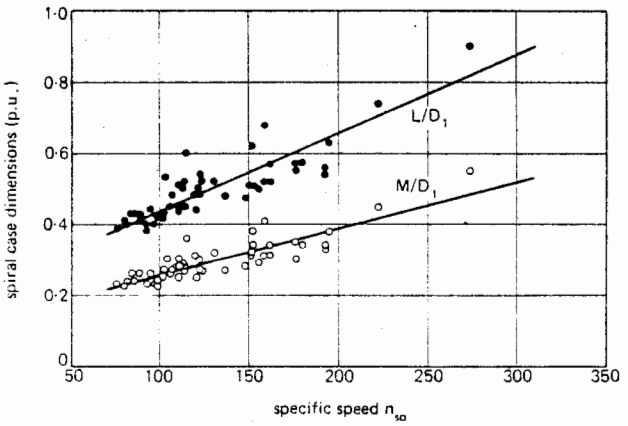

Fig. 21. Main spiral casing dimensions versus specific speed as pump.

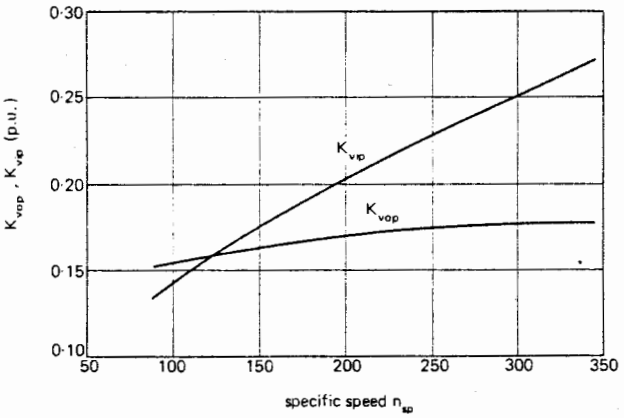

Fig. 22. Ratio between actual and spouting velocities at spiral casing outlet and at runner inlet in pumping mode versus specific speed as pump.

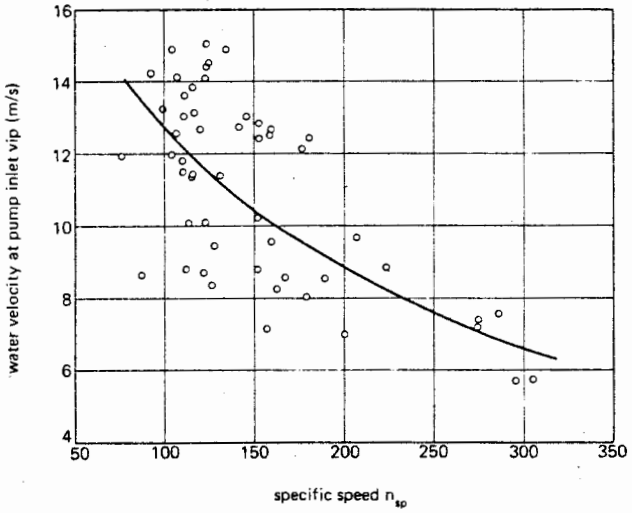

Fig. 23. Water velocity at the runner inlet in the pumping mode versus specific speed as pump.

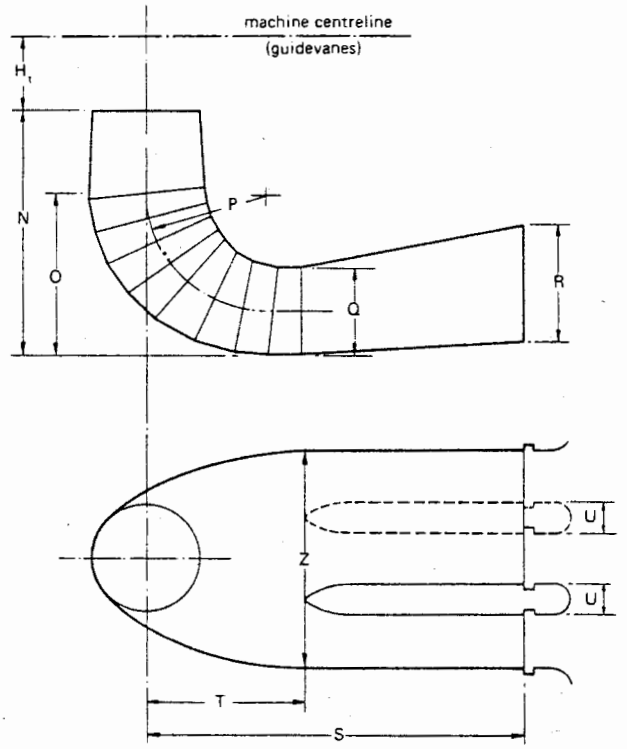

Fig. 24. Main draft tube dimensions.

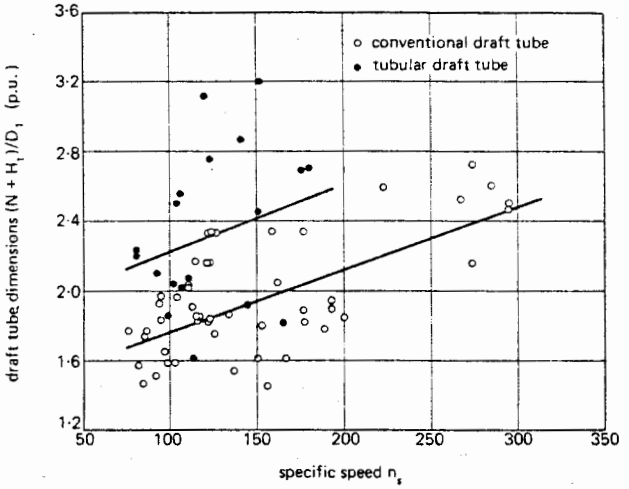

Fig. 25. Main draft tube dimensions $(N + H_t)/D_1$ versus specific speed as a pump.

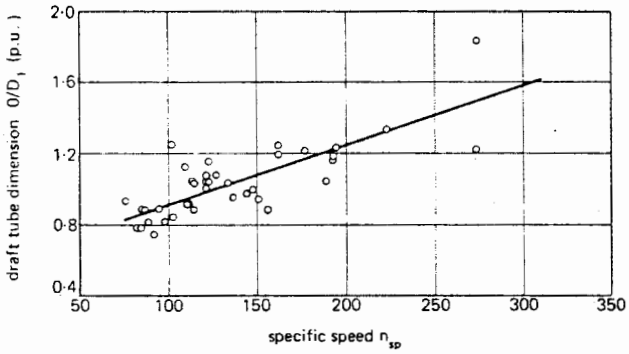

Fig. 26. Main draft tube dimensions O/D, versus specific speed as a pump.

Fig. 23 gives the mean statistical value of this velocity v_{ip} versus the specific speed n_{sp}. The interpolating function is:

$$v_{ip}=1/(0.043+0.000355\ n_{sp})$$

where:

r=0.73 s=2.06

The comparison with the water velocity at the runner discharge of conventional Francis turbines[1] leads to similar findings as for the spiral case in the preceding chapter.

The most important dimensions of the draft tube indicated in Fig. 24 are given by Figs. 25 to 33.

The interpolating functions for the different curves are as follows:

$$(N+H_t)/D_1=1.42+0.0035\ n_{sp}$$

conventional draft tubes

r=0.65 s=0.25

$$(N+H_t)/D_1=1.84+0.0039\ n_{sp}$$

tubular draft tubes

r=0.26 s=0.45

$$O/D_1=0.57+0.00033\ n_{sp}$$

r=0.78 s=0.13

$$P/D_1=0.42+0.0026\ n_{sp}$$

r=0.75 s=0.10

$$Q/D_1=0.37+0.00094\ n_{sp}$$

conventional draft tubes

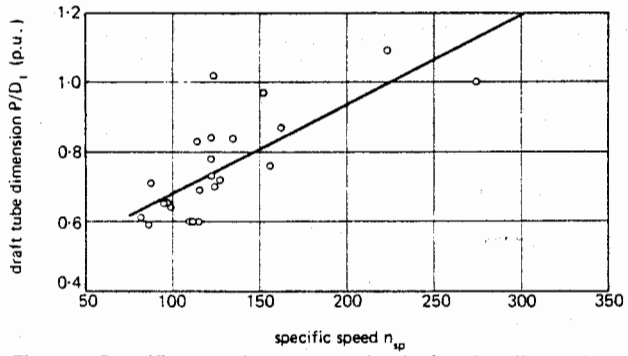

Fig. 27. Specific speed versus main draft tube dimensions P/D_1 *— pumping mode.*

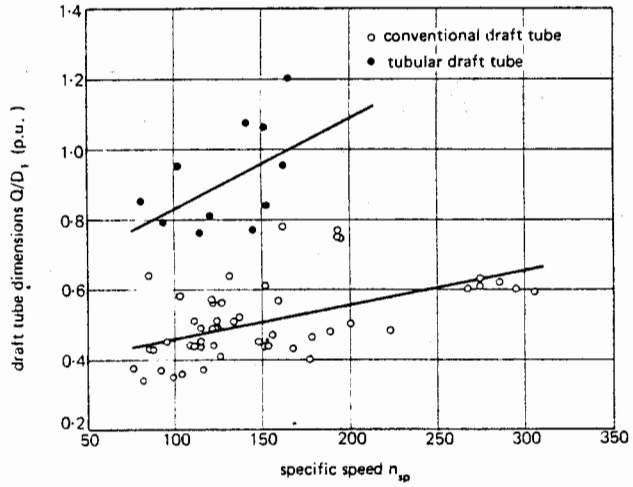

Fig. 28. Specific speed versus main draft tube dimensions Q/D_1 *— pumping mode.*

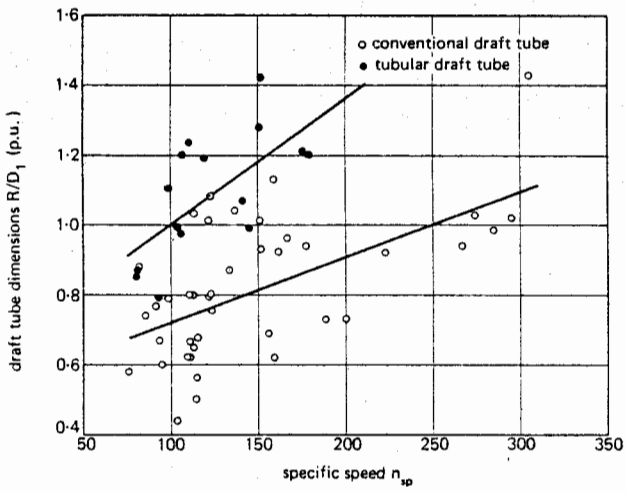

Fig. 29. Specific speed versus main draft tube dimensions R/D_1 *— pumping mode.*

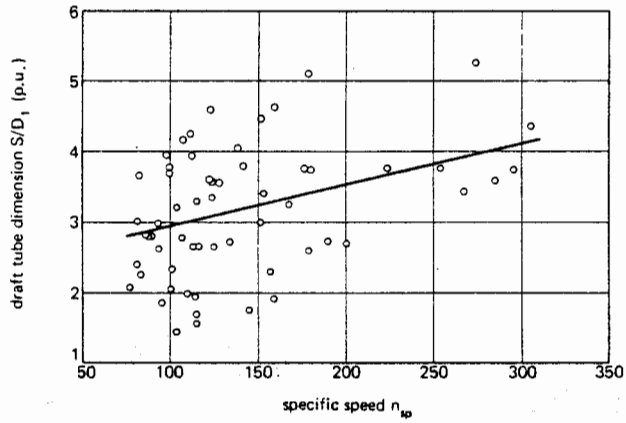

Fig. 30. Specific speed versus main draft tube dimensions S/D_1 *— pumping mode.*

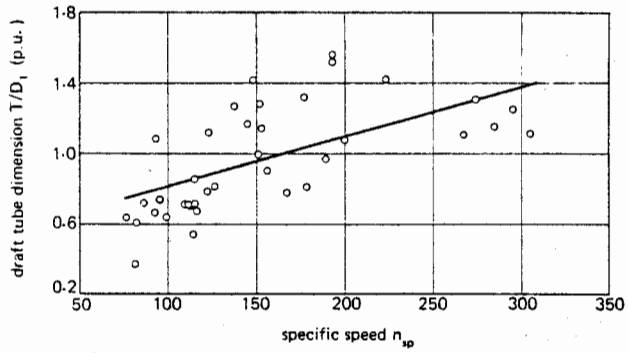

Fig. 31. Specific speed versus main draft tube dimensions T/D_1 *— pumping mode.*

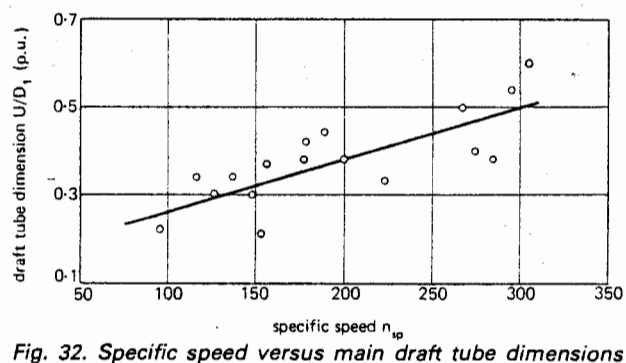

Fig. 32. Specific speed versus main draft tube dimensions U/D_1 *— pumping mode.*

r=0.50 s=0.095

$$Q/D_1=0.57+0.0026\ n_{sp}$$

tubular draft tubes

r=0.53 s=0.13

$$R/D_1=0.54+0.0019\ n_{sp}$$

conventional draft tubes

r=0.60 s=0.16

$$R/D_1=0.64+0.0036\ n_{sp}$$

tubular draft tubes

r=0.66 s=0.13

$$S/D_1=2.32+0.0059\ n_{sp}$$

r=0.38 s=0.84

$$T/D_1=0.55+0.0028\ n_{sp}$$

r=0.60 s=0.22

$$U/D_1=0.15+0.0012\ n_{sp}$$

r=0.78 s=0.066

$$Z/D_1=-0.083+0.012\ n_{sp}$$

r=0.90 s=0.29

The figures show that for increasing values of n_{sp} the draft tube dimensions, and particularly its developed length related to the S and $(N+H_t)$ values, decrease when referred to the runner diameter D_6 taken from Fig. 9. On the other hand, for increasing values of n_{sp}, the ratio K_{vip}, the inlet velocity of the runner to spouting velocity relative to the rated head, increases as shown in Fig. 22.

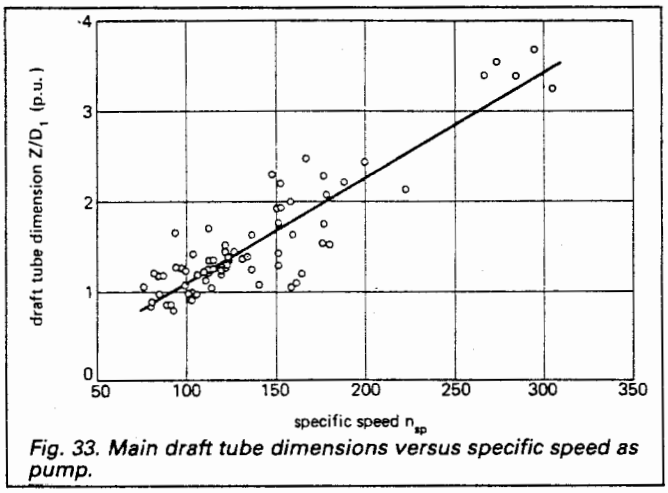

Fig. 33. Main draft tube dimensions versus specific speed as pump.

These findings are the same as obtained for conventional Francis turbines.

Conclusions

The present investigation shows only a limited scattering of data for most of the curves drawn, particularly those associated with the peripheral velocity coefficient and the runner dimensions.

The number of powerplants studied and the consideration given to the operating head ranges has made it possible to develop a method of calculation which allows the sufficiently accurate preliminary sizing of a reversible pump-turbine, within the limits stated in the text. □

Acknowledgments

The Authors wish to thank all the manufacturers indicated in Table I for supplying the main design data and dimensions of their machines, which has made possible the present study.

Manuscript received in May 1979.

References

1. DE SIERVO, F. AND DE LEVA, F. "Modern Trends in Selecting and Designing Francis Turbines", *Water Power & Dam Construction*; August 1976.
2. DE SIERVO, F. AND DE LEVA, F. "Modern Trends in Selecting and Designing Kaplan Turbines", *Water Power & Dam Construction*; December 1977.
3. DE SIERVO, F. AND LUGARESI, A. "Modern Trends in Selecting and Designing Pelton Turbines", *Water Power & Dam Construction*; December 1978.

Bibliography

MEIER, W., MÜLLER, J., GREIN, H., JAQUET, M. "Pump-Turbines and Storage Pumps", *Escher Wyss News*, 1971/2.

SONO, M., FUKUMASU, K., WATANABE, T., MUTAGUCHI, K. "Design and Manufacture of Francis Type Reversible Pump Turbines", *Mitsubishi Technical Review*; February 1977.

ALESTIG, R., MCHAMISH, G. "Development of High Head Single Stage Reversible Pump-Turbines", Joint Symposium ASCE-IAHR/AIRH-ASME, Fort Collins, Colorado, USA 1978.

KIMURA, Y., YOKOYAMA, T. "Planning of Reversible Francis Pump-Turbine", *Hitachi Review* Vol. 22, No. 8. 1973.

CERAVOLA, O., MALGUORI, E. "Italian Achievement in Pumped Storage Projects with Pump-Turbines. Present and Future Trends", Pump-Turbine Schemes Planning, Design and Operation, ASME-CSME; Niagara Falls New York. Joint Conference, USA; 1979.

GREASER, J.-E. "Abaque pour Pompes et Pompes-Turbines Reversibles", Joint Symposium ASCE-IAHR, 1978.

GULI, FR. P. "The European Pump-Turbines Minimum Suction Head", Conference on Fluid Machinery, Budapest, Hungary; September 1972.

FUKASU, S., TAZUKE, O. AND HIROYOSHI, H. "Recent Trends in Hydroelectric Power Station Equipment", *Hitachi Review; Special issue, No. 13*

KAUFMANN J. P. "The Dimensioning of Pump-Turbines", *Water Power & Dam Construction*; August and September 1977.

CHAPPUIS, J. "Quelques Considérations dans le Cadre de notre Programme de Recherche sur le Pompes-Turbines", *Bulletin Technique Vevey*; 1970.

FUKASU, S. "Trends of Pumped Storage Equipment", International Conference on Pumped Storage Development and its Environmental Effects, University of Wisconsin, USA; September 1971.

WARNOCK, J. G. "Trends Established from 20 years of Modern Pumped Storage Practice and for the Future", International Conference on Pumped Storage Development and its Environmental Effects, University of Wisconsin, USA; September 1971.

Dams and their tunnels

By A. M. Muir Wood, W. H. Cooper and B. C. Kidd†
Partner* and Consultant*

PART FOUR

The final part of the article is concerned principally with linings and monitoring, and provides readers with a comprehensive bibliography.

ACCESS ADITS and the construction of shafts associated with tunnels were discussed at the end of last month's article. Before going on to linings, the authors describe some of the problems associated with submerged intakes.

Submerged intakes

Where a deep lake is being used as a storage reservoir it may be of considerable economic advantage to utilize the existing storage capacity by drawing down below the present water level. This can of course be accomplished by excavating a channel through the original outflow point but frequently it is more satisfactory to create a new low-level draw-off point by tunnelling under the banks of the reservoir to within a short distance of the water surface and eventually blasting away the intervening rock mass. Before undertaking an operation of this nature a thorough geological investigation is necessary to ensure that the rock, in the area where the submerged intake is planned, is reasonably sound and, if not free from fissures, at least capable of being grouted to make it watertight.

Excavation towards the lake bed must be carried out carefully with drilling and grouting ahead to make sure that there is no uncontrolled leakage into the tunnel from the reservoir. The length of rockplug which must be left will depend on the quality of the rock, the depth of water above and the diameter of the approach tunnel. This operation is only practical where a rock surface clear of soft material is located in the lake bed.

When the tunnel has been taken to its nearest point to the water surface it is usual to excavate an enlargement in the tunnel floor so that any rock debris from the final blast will be trapped there and not cause any constriction in the water flow through the tunnel.

When the charge has been water-proofed and made ready the tunnel downstream of the rock plug should then be flooded. The water will act as a cushion to prevent much muck being thrown into the tunnel itself and if there is a suitably located shaft the effect of the blast will largely

* Sir William Halcrow & Partners, Newcombe House, 45 Notting Hill Gate, London W11.
† B. C. Kidd, formerly of the same organisation, died on 31st January 1978 after making a major and thorough contribution to the content, structure and drafting of the article.